AGU PUBLICATIONS

JGR

Journal of Geophysical Research: Oceans

RESEARCH ARTICLE

10.1002/2014JC009911

Key Points:
- We define new metrics of AWP variations
- The rainy season variations are related to new AWP metrics
- Atlantic TC activity is related to onset of AWP

Correspondence to:
V. Misra,
vmisra@fsu.edu

Citation:
Misra, V., H. Li, and M. Kozar (2014), The precursors in the Intra-Americas Seas to seasonal climate variations over North America, *J. Geophys. Res. Oceans*, *119*, 2938–2948, doi:10.1002/2014JC009911.

Received 14 FEB 2014
Accepted 21 APR 2014
Accepted article online 25 APR 2014
Published online 14 MAY 2014

The precursors in the Intra-Americas Seas to seasonal climate variations over North America

Vasubandhu Misra[1,2,3], H. Li[1,2], and M. Kozar[1,2]

[1]Department of Earth, Ocean and Atmospheric Science, Florida State University, Tallahassee, Florida, USA, [2]Center for Ocean-Atmospheric Prediction Studies, Florida State University, Tallahassee, Florida, USA, [3]Florida Climate Institute, Florida State University, Tallahassee, Florida, USA

Abstract In this paper, we show from observations that the Intra-American Seas precursor as characterized by the onset of the Atlantic Warm Pool (AWP; defined by the area enclosed by 28.5°C isotherm in the tropical Atlantic Ocean) has discernible impact on the boreal summer and fall seasonal climate variations over North America, a season and a region well known for relatively poor seasonal predictability. The onset of the AWP season is objectively defined as the day when the daily anomaly of the AWP area, west of 50°W, and north of the equator exceeds its climatological annual mean value. We show that early (late) onset of AWP is associated with following August-September-October (ASO) deficit (excess) seasonal rainfall anomalies over southern Mississippi valley extending to the Midwest US east of Iowa. On the other hand, Central America and the Caribbean region exhibit enhanced (decreased) ASO seasonal mean rainfall during an early (late) onset of AWP. We also find that early (late) onset of the AWP is associated with early (late) onset and early (late) demise of the rainy season over Mesoamerica. This relationship also leads to association of early (late) onset of AWP with increased (shortened) length of the rainy season over Mesoamerica. These teleconnections are dictated by the modulation of the low-level flow and moisture flux convergence associated with the varying development of the AWP. Similarly, we find that early (late) onset years of the AWP are associated with a more active (inactive) seasonal Atlantic tropical cyclone activity. These teleconnections are sustained from the fact that the AWP onset date variations are found to be a precursor to the seasonal AWP size variations.

1. Introduction

The Atlantic Warm Pool (AWP) was first noted in *Weisberg* [1996] as part of the western hemisphere warm pool region that included eastern north Pacific region, the Gulf of Mexico, the Caribbean Sea, and the western tropical north Atlantic Ocean. This warm pool region has since been extensively investigated [e.g., *Wang and Enfield*, 2001; *Wang et al*., 2006]. *Wang et al*. [2008a] indicated that the variations of the AWP dominated the variability of the western hemisphere warm pool. Therefore, in this study, we lay emphasis on characterizing the AWP part of the western hemisphere warm pool.

Most studies on the subject of AWP variability have focused on seasonal anomalies of the August-September-October (ASO) AWP area, which is typically defined as the area covered by Sea Surface Temperatures (SSTs) warmer than a critical value (usually 28.5°C) in the Intra-American Seas. The definition of the size of the AWP is hinged to the area enclosed by the 28.5°C isotherm because it displays the strongest interannual variations compared to the variations by areas of other isotherms that commonly appear in the Intra-American Seas region [*Misra and DiNapoli*, 2013]. Furthermore, with this definition of AWP, several interesting teleconnections associated with APW variability have been shown [*Wang and Enfield*, 2003, *Wang et al*.2006, 2008a, 2008b; *Misra et al*., 2011]. For example, *Wang et al*. [2006] find years with large seasonal mean AWP area are associated with a weakened north Atlantic subtropical high and increased atmospheric convection and cloud cover over the AWP region. As a result, this corresponds to a weak tropospheric vertical wind shear and a deep warm upper ocean, thus increasing seasonal Atlantic tropical cyclone activity. The opposite is true of an anomalously small AWP, wherein, it is associated with a strengthened subtropical high. Similarly, *Misra et al*. [2011] find that in years when the seasonal mean of the AWP is anomalously large, the sea breeze over the Florida panhandle becomes weaker because of the prevailing anomalous meridional large-scale flow forced by the movement of the north Atlantic subtropical high. Likewise, *Wang et al*. [2008a] indicate that in years of large seasonal mean AWPs, the Caribbean low-level jet and the southerly Great Plains low-level jet is weakened, which consequently reduces the net moisture transport in the lower atmosphere

resulting in reduced rainfall over these regions. Once again, the opposite is true of anomalously small seasonal AWPs, wherein they are associated with a stronger jets and enhanced rainfall in the region.

Wang and Enfield [2001], *Lee et al*. [2007], and *Misra et al*. [2012] found that these AWP areal variations are dominated by surface heat flux variations, with cloud radiative feedbacks on downwelling shortwave and net long wave flux dominating over other heat flux terms. Several earlier studies [*Wang et al*., 2010; *Misra and DiNapoli*, 2012; *Lee et al*., 2013] allude to an interhemispheric teleconnection involving the AWP. *Wang et al*. [2010] and *Lee et al*. [2013] suggest that the seasonal march of the atmospheric convection related to the Atlantic Inter-Tropical Convergence Zone (ITCZ) from the Amazon in the boreal winter to the Intra-Americas Seas in the boreal summer helps to regulate an overturning interhemispheric meridional (Hadley) circulation. In fact, *Misra and DiNapoli* [2012] suggest from their observational study that convection over equatorial Amazon leads the variations of SST over the Intra-Americas Seas by nearly two seasons by way of regulating the meridional migration of the western Atlantic ITCZ.

The Mesoamerican region that includes central Mexico, Belize, Guatemala, El Salvador, Honduras, Nicaragua, and northern Costa Rica is characterized by a distinct seasonal rainfall season. The region has a double precipitation maxima during the summer wet season that cradles a relative minimum during July-August, which is often termed as the Mid-Summer Drought [MSD; *Magaña et al*., 1999]. The MSD has been widely studied from observations [*Magaña et al*., 1999; *Mapes et al*., 2005; *Small et al*., 2007; *Magaña and Caetano*, 2005] and model diagnostics [*Diro et al*., 2012]. A widely known but contentious theory for this MSD phenomenon is the lagged response of the precipitation in Mesoamerica to a similar bimodality in the northeast Pacific SST [*Magaña et al*., 1999]. They show that northeast tropical Pacific SST displays two maximas, one in May and another in August, each prior to the precipitation maximas in June and September over Mesoamerica [*Magaña et al*., 1999]. Alternative theories for MSD have been also been proposed for which the readers are referred to *Mapes et al*. [2005], *Magaña and Caetano* [2005], *Kelly and Mapes* [2011], and *Karnauskas et al*. [2013].

This study introduces an objective way of determining the onset of the AWP, which has a potential advantage of being a harbinger of the future seasonal evolution of the AWP and its impact on the boreal summer and fall season climate over the United States and Mesoamerica.

2. Methodology and Data Sets

We extend a concept used successfully in the context of the monsoon rainy season [*Liebmann et al*., 2007; *Misra and DiNapoli*, 2013] to define objectively the onset, demise, and the length of the AWP season. We define daily anomalous area of AWP ($D'_m(n)$) for a given year m and day n as:

$$D'_m(n) = C_m(n) - \bar{\bar{C}} \tag{1}$$

where, m is the year which in our study ranges from 1979 to 2012, C_m (n) is area of AWP on day n of the mth year and $\bar{\bar{C}}$ is the climatological annual mean average of the area of the AWP. Then, we define the cumulative anomalous area of AWP ($C'_m(n)$) as:

$$C'_m(n) = \sum_{i=1}^{n} \{D'_m(i)\} \tag{2}$$

where, the accumulation is carried out from i = 1 (for January 1) and i = n for the nth day of the mth year. An example of the daily time series of $C'_m(n)$ is shown in Figure 1 for year (m=) 2002. The onset date of the AWP season is objectively defined as the first date when $C'_m(n)$ is above the climatological mean ($\bar{\bar{C}}$; see Figure 1) and appears west of 50°W and north of the equator. The latter condition is dictated to ensure that the onset of AWP is not declared from warm anomalies appearing in the eastern Atlantic Ocean. The value of $C'_m(n)$ (see equation 1) from beginning of January 2002 to say beginning of July 2002 (Figure 1) is expectedly going to be increasingly negative as it covers a period when the daily area of the AWP is insignificantly small compared to the climatological annual mean. For example, in Figure 1 on day 1 (=1 January 2002), C'_{2002} (1) is -2×10^6 km^2 (since C_{2002} (1) = 0) and in day 2 (2 January 2002), C'_{2002} (2) is -4×10^6 km^2 (since C_{2002} (2) = 0), and so on. By Julian day 183 (2 July 2002; Figure 1), we get the first positive value of D'_{2002}

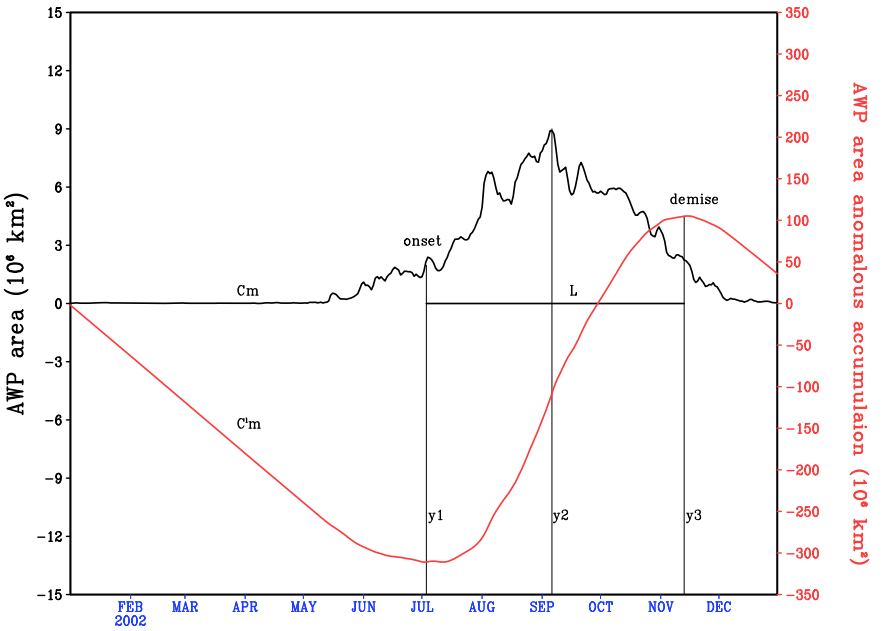

Figure 1. A schematic showing the AWP variants like the onset date (y_1), demise date (y_3), length in days (L), and peak date (y_2) of the AWP season on a given observed time series of the anomalous accumulation (C'_m; see equation 1 in text; in black) computed from the daily area of the AWP (C_m; in red) for say year 2002.

(183)=0.12 × 10^6 km^2, which marks the first date when the daily mean area of AWP exceeds the corresponding climatological annual mean value of 2.00 × 10^6 km^2. This makes the cumulative anomalous area ($C'_m(n)$) to rise from its minimum value (Figure 1). Similarly, the objective diagnosis of the demise date of the AWP season is defined when $C'_m(n)$ is maximum (see Figure 1). So in 2002 for example, the demise date is 319 Julian day (or November 15th; Figure 1). On this day, the D'_{2002} (319) value is −0.04 × 10^6 km^2 (when it begins to recede below, the corresponding climatological annual mean value) and the C'_{2002} (319) value is 105.17 × 10^6 km^2. It should be noted that at the time of the demise of the AWP the accumulated anomalies are maximum as the accumulation is completed over the entire AWP season.

We can also define the length of the AWP season (L(m)) for a given year m as:

$$L(m)=y_3(m)-y_1(m) \tag{4}$$

where, y_3(m) and y_1(m) are the demise and onset dates of the AWP season in year m (see Figure 1). The peak date of the AWP season is defined as the date in the season of the year when the area of the AWP is the largest.

Rainfall data are obtained via the Climate Prediction Center (CPC) Unified Gauge-Based Analysis of Global Daily Precipitation on a 0.5° degree grid [*Chan et al*., 2008]. We also made use of the National Centers for Environmental Prediction (NCEP) Climate Forecast System Reanalysis [CFSR; *Saha et al*., 2010], which is regarded as "coupled" ocean-land-atmosphere reanalysis for mean sea level pressure, 925 hPa winds, atmospheric moisture, daily SST. It is noted that the CFSR SST is strongly nudged to the observed daily SST [*Saha et al*., 2010]. In computing the statistical significance of the correlations, we follow the nonparametric test of bootstrapping technique [*McClave and Dietrich*, 1994; *Efron and Tibshirani*, 1993]. In this method, the pair of time series is resampled 1000 times randomly (with replacement). The correlations of the true pair of time series are then considered to be significant at 90% confidence interval if it lies within the 5th or beyond the 95th percentile of the distribution of the 1000 correlations of the randomly shuffled time series.

3. Results

3.1. Climatological Features

The climatological SST at onset of the AWP season (y_1 in Figure 1) is shown in Figure 2a. At this time of the AWP season, the warm pool with SST's in excess of 28.5°C is located over the Caribbean Sea between Cuba

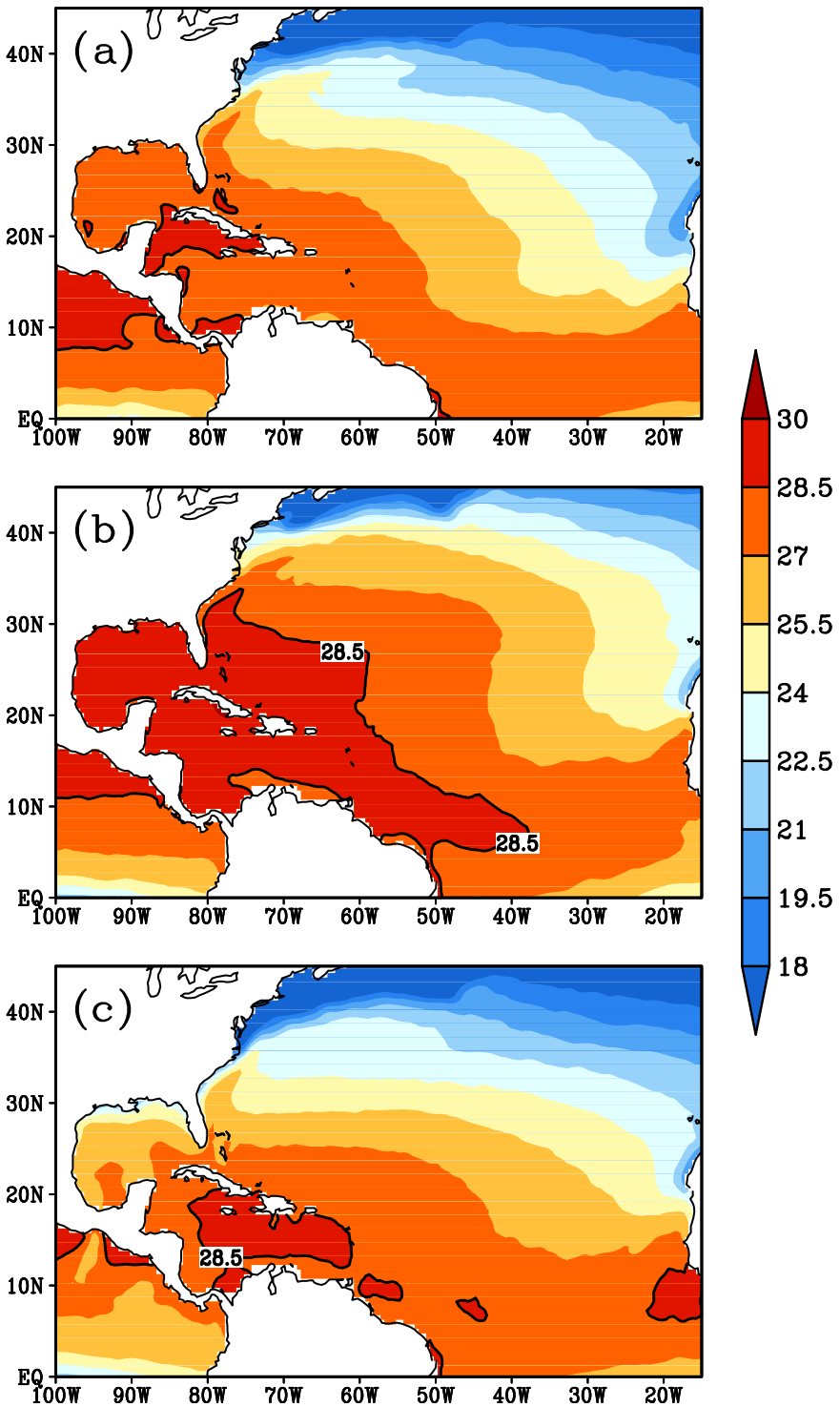

Figure 2. The climatological mean SST (°C) at (a) time of onset, (b) peak, and (c) time of demise of AWP season. The corresponding 28.5°C isotherm is contoured in each of the panels.

and the Yucatan peninsula. At the time of the peak of the AWP season (y_3 in Figure 1), the climatological SST in Figure 2b shows that the warm pool is fully established over the Gulf of Mexico, Caribbean Sea, parts of the northwest tropical Atlantic, and over the deep tropical Atlantic extending as far east as 40°W. Similarly, the climatological distribution of SST at the time of the demise of the AWP season (y_2 in Figures 1 and 2c) is characterized by the confinement of the warm pool to within the Caribbean Sea. In comparing Figures

2a–2c, it is apparent that there is significant warming (cooling) in the Gulf of Mexico and mid-Atlantic Ocean of 2–3°C with comparatively more gradual (warming) cooling of around 1°C in the Caribbean Sea during the growth (decay) phase of the AWP season.

3.2. Interannual Variations of the AWP

The time series of the anomalies of the onset date, demise date, length, growth, and demise rates of the AWP season are shown in Figure 3 with their corresponding standard deviation. It is seen that the variability of the onset date ($\sigma \sim$18 days; Figure 3a) is comparable to that of the demise date ($\sigma \sim$17days; Figure 3c) while the variability of the peak date is smaller by about 6 days ($\sigma \sim$11 days; Figure 3b). The variability in the length of the AWP season is comparably large ($\sigma \sim$31 days; Figure 3c) as it is affected by the variations of the onset and demise date of the AWP season. A linear trend in the onset (Figure 3a) and demise dates (Figure 3b) is evident. However, we are skeptical of removing this trend from the relatively short data record of 34 years.

The correlations (ρ) between the anomalies of the onset date, demise date, length of the AWP season, and the mean area of AWP over the length of the AWP season are shown in Table 1. We find that the longer length of the AWP season (L) is determined usually by the simultaneous occurrence of early onset and late demise of the AWP. These correlations also suggest that years with anomalously large (small) area of the seasonal AWP are associated with an early (late) onset, late (early) demise, and thus a longer (shorter) AWP season.

3.3. Impact on the Seasonal Climate Variations over the United States

We have correlated the onset of the AWP season with ASO seasonal mean rainfall anomalies over North America and northern parts of South America in Figure 4. Figure 4 clearly shows that seasonal rainfall variability in the summer and fall seasons are significantly modulated by the onset date variations of the AWP season. This is not surprising given from the discussion in the previous subsection that the onset of the AWP is significantly related to the seasonal variability of the area of the AWP. *Wang et al*. [2006] point that years with large AWP area in the ASO season are characterized by corresponding excess of seasonal rainfall over Central America and Caribbean, and reduced rainfall in the Midwestern United States. However, the advantage of finding this teleconnection with the onset of the AWP season allows it to be leveraged for operational seasonal forecasting as the onset precedes the season. This teleconnection manifests from the modulation of the moisture transport, which is largely from the associated variability of the low-level winds that results in the weakening (strengthening) of the southerly flow from the Gulf of Mexico and easterly flow over the Caribbean region [*Wang et al*. 2006] during large (small) AWP years. This is corroborated in Figure 5, which shows the correlation of the Mean Sea Level Pressure (MSLP), divergence of vertically integrated moisture flux with onset date of AWP, and the regression of the 925hPa winds on the onset date of the AWP. Figure 5 suggests that early onset of AWP is associated with weaker easterlies and southerlies in the Caribbean and the Gulf of Mexico in the ASO season. Furthermore, the north Atlantic subtropical high undergoes similar modulation with it weakening during early onset of AWP years. Figure 5 also shows that early onset is characterized by moisture flux convergence over Central America and Caribbean region while moisture flux divergence occurs in the Southern Mississippi valley to Midwest US east of Iowa. The opposite is true of late AWP onsets, which are associated with a stronger subtropical high, and are characterized by moisture flux convergence over the east-central US.

3.4. Impact on North Atlantic Tropical Cyclone Activity

The variability of the onset date of the AWP is also associated with variability of annual Atlantic tropical cyclone frequency (Figure 6a). The shared variance between annual TC counts and AWP onset date is in fact higher than that between peak-season ENSO variability on the number of Atlantic tropical cyclones (Figure 6b), but lower than the shared variance between TC frequency and Maximum Development Region (MDR; 6–18°N 20–60°W) SST variability (Figure 6c). Figure 6a suggests that early (late) onset of the AWP is characterized by larger (smaller) number of Atlantic tropical cyclones. Table 2 shows that late (early) onset date of the AWP is closely associated with cold (warm) MDR SST anomalies and fewer (more) Atlantic tropical cyclones and hurricanes. *Wang and Lee* [2007] indicate that large AWPs reduce the low-level easterly winds and the upper level westerly winds, thereby reducing the vertical wind shear in the AWP region and creating an environment that fosters Atlantic tropical cyclogenesis. Furthermore, the onset date of AWP is relatively poorly correlated with the ENSO index of the Niño3.4 SST anomalies. But most importantly, Figure 6 and

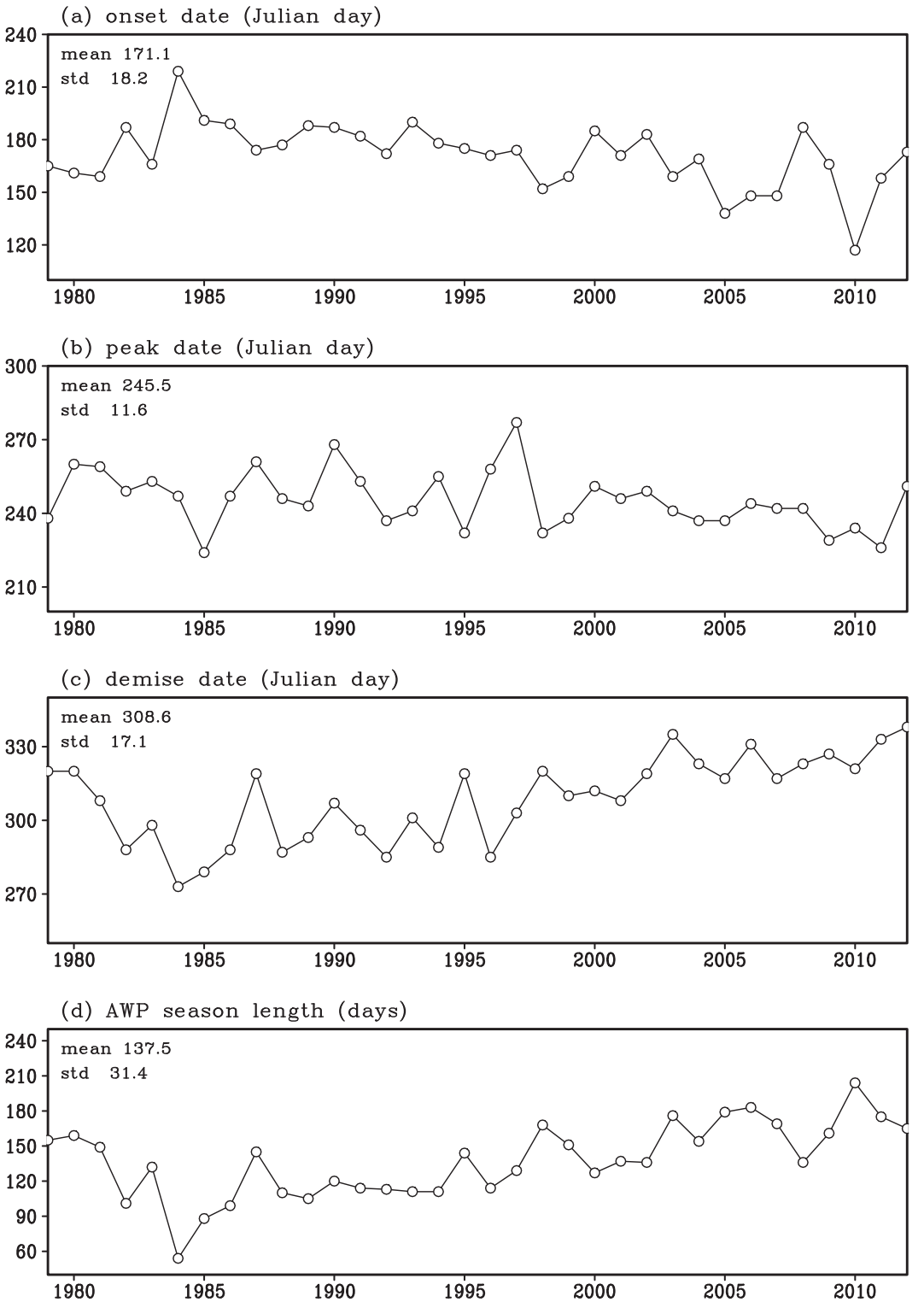

Figure 3. The time series of (a) onset date (in Julian day), (b) peak date (in Julian day), (c) demise date (in Julian day), and (d) length of the AWP season (in days) of the AWP season (in Julian day). The standard deviation and the mean of the time series are indicated in the top left corner of each panel.

Table 2 point to a potential advantage of monitoring the onset of the AWP, which leads the Atlantic tropical cyclone season, especially in years when early onset of AWP occurs. The other two metrics of ENSO index and MDR SST anomalies are contemporaneous to the Atlantic tropical cyclone season. This is best illustrated

Table 1. Correlations of the AWP Onset Date With Other AWP Variants[a]

	Onset Date (y_1)	Demise Date (y_3)	Length of AWP Season (L)	Seasonal Areal Average of AWP
Onset	1	−0.58	−0.89	−0.71
Demise	−0.58	1	0.88	0.82
Length	−0.89	0.88	1	0.86

[a]Those that pass the significance test at 10% significance level are in bold.

for the highly anomalous season of Atlantic tropical cyclone activity in 2005 (28 named storms), when the onset date was May 18, which is significantly earlier than the climatological onset date of June 20 (Figure 3a).

Our further diagnosis reveals that this association of onset date variability of AWP with Atlantic tropical cyclone activity is unrelated to variations of the tropical cyclone activity in the early part of the season or variations of the tropical cyclone activity within the western tropical Atlantic Ocean because of any implied preconditioning of the SST's in the Intra-American Seas. The diagnosed relationship shown in Figure 6a is largely a manifestation of the relationship of the variability of the onset of the AWP season to the area of the AWP, which affects the vertical shear in the maximum development region of the tropical Atlantic Ocean [*Wang and Lee*, 2007, *Wang et al*., 2008a].

3.5. Impact on Mesoamerican Seasonal Climate

As pointed in Figure 5, the variability of the onset date of the AWP season has an associated variability on the easterly flow over the Caribbean Sea, which will potentially influence the gap winds through the Gulfs of Papagayo and Panama [*Xie et al*., 2005]. In a related study, *Magaña and Caetano* [2005] proposed that the SST modulated by the gap winds, which are in turn associated with the variations in the Caribbean Low-Level Jet (CLLJ) affect the tropical convective activity over the Mesoamerican region. In Figure 7, we show the correlation of onset date of the AWP season with the onset date, demise date, and length of the rainy season in Mesoamerica, which were calculated in exactly the same way as illustrated in Figure 1.

The positive correlations in Figure 7a indicate that early (late) onset of the AWP season is associated with early (late) onset of the rainy season over Mesoamerica. This relationship is also associated with stronger

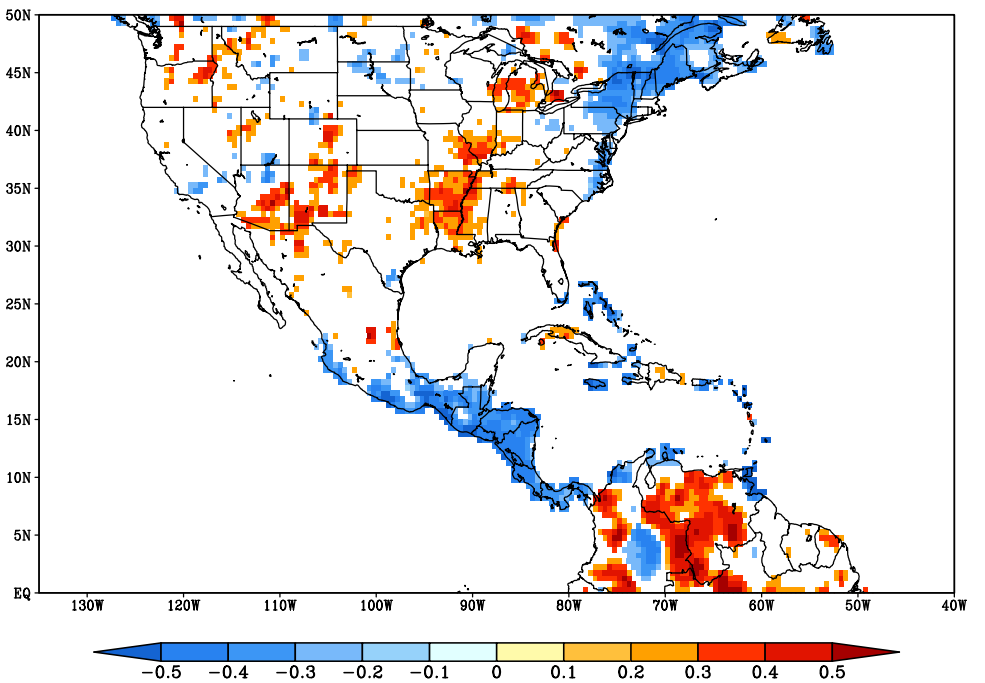

Figure 4. The correlation of variability of onset date of AWP with the August-September-October seasonal mean rainfall anomaly over North America over land. Only significant values at 90% confidence interval are shaded.

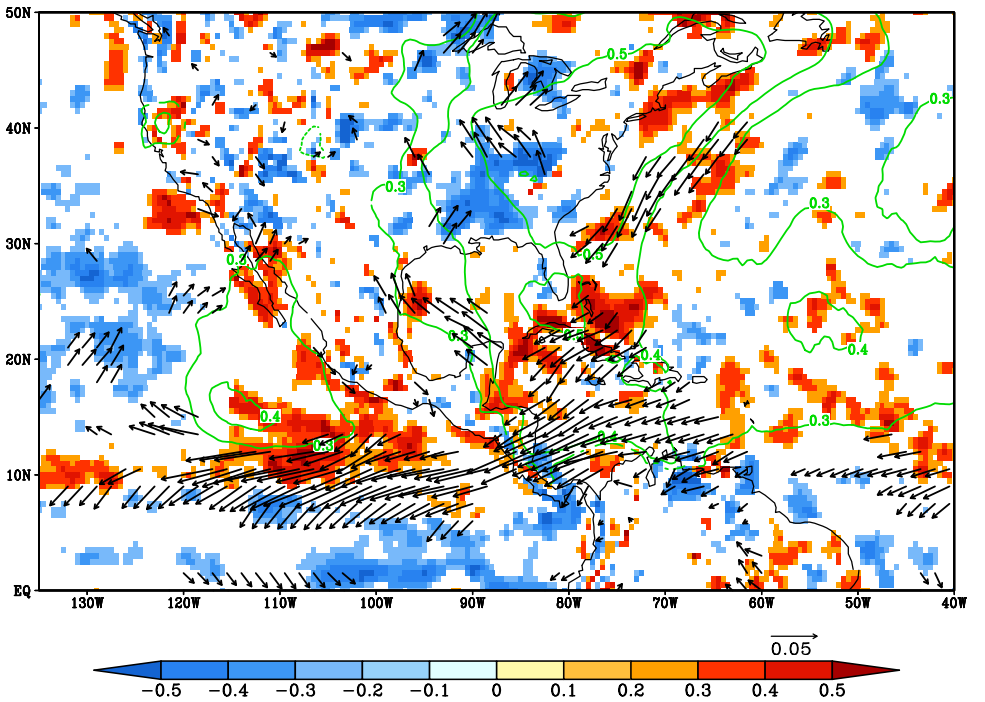

Figure 5. Correlation of the variability of the onset date of the AWP season with ASO seasonal mean MSLP (contour), and vertical integrated moisture flux convergence (shaded). Regression of the 925hPa winds on the onset date of the AWP (vector). Only significant values at 90% confidence interval are shown.

(weaker) moisture convergence at the time of early (late) onset of the rainy season over Mesoamerica and weaker (stronger) easterlies over the Caribbean Sea (not shown but akin to Figure 5, which is for the ASO season). Similarly, the positive correlation in Figure 7b suggests that early (late) onset of the AWP season is associated with early (late) demise of the rainy season over Mesoamerica. In contrast to Figures 7a and 7b, the correlations of the length of the rainy season over Mesoamerica with the onset date of the AWP season are weaker and negative in Figure 7c, which is largely on account of relatively smaller variations in the total length of the rainy season. There are two reasons on why Figure 7c has negative correlations:

1. Early (late) onset of AWP is associated with longer (shorter) AWP season and larger (smaller) AWP seasonal mean area (Table 1). As a result, it influences the low-level flow and the corresponding moisture flux convergence to modulate the length of the rainy season over Mesoamerica (not shown) in such a way to give rise to the negative correlations in Figure 7c. For example, in a large AWP year, the low-level easterly flow over the Caribbean Sea becomes weak (akin to Figure 5) and results in stronger moisture flux convergence over Mesoamerica, coinciding with early onset of the rainy season.

2. The variation of the onset date (Figure 7d) of the rainy season of Mesoamerica is larger than that of the demise date (Figure 7e), which gives rise to corresponding increase in the standard deviation of the length of the rainy season (Figure 7f). Therefore, their modulation by variations of the onset date of the AWP is correspondingly larger (smaller) for the onset (demise) date variations of the rainy season over Mesoamerica, giving rise to the negative correlations in Figure 7c.

4. Discussion and Conclusions

In this paper, we have introduced a novel metric of the onset of the AWP season that could potentially be the harbinger for the forthcoming rainy season over major parts of North America. The onset date of the AWP season is determined objectively as the day when the daily anomalous accumulation of the AWP area exceeds the climatological mean of the AWP area and appears west of 50°W and north of the equator. The variability of this onset date is found to be associated with the seasonal anomalies of the area of the AWP season; this relationship of the onset date of the AWP season sustains the display of its teleconnection with

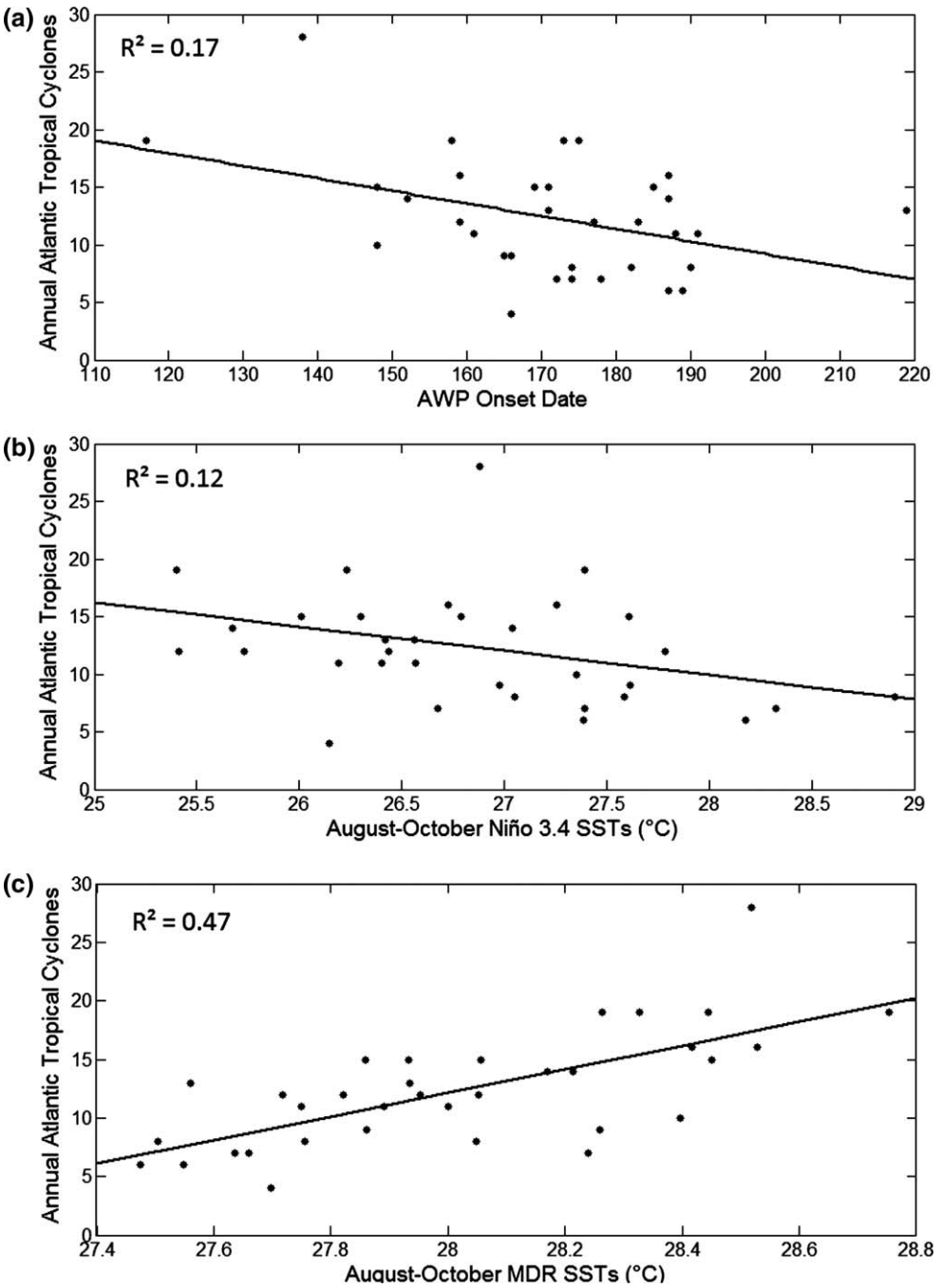

Figure 6. The relationship of the total number of Atlantic tropical cyclones with (a) the variability of the onset date of the AWP, (b) the ENSO variability, and (c) the influence of the SST variability in the MDR (6–18N and 20–60W) in the deep tropical Atlantic. The R^2 values are statistically significant in all three cases at 90% confidence interval.

Table 2. Correlations of the AWP Onset Date With Remote and Local SST Anomalies[a]

	Onset Date of AWP
MDR SST anomalies (area averaged over 6°–18°N and 20°–60°W; averaged August-September-October)	**−0.61**
Niño3.4 SST anomalies (averaged August-September-October)	0.28
Atlantic TC's	**−0.41**
Atlantic hurricanes	**−0.47**

[a]Bold values are significant at 10% significance level.

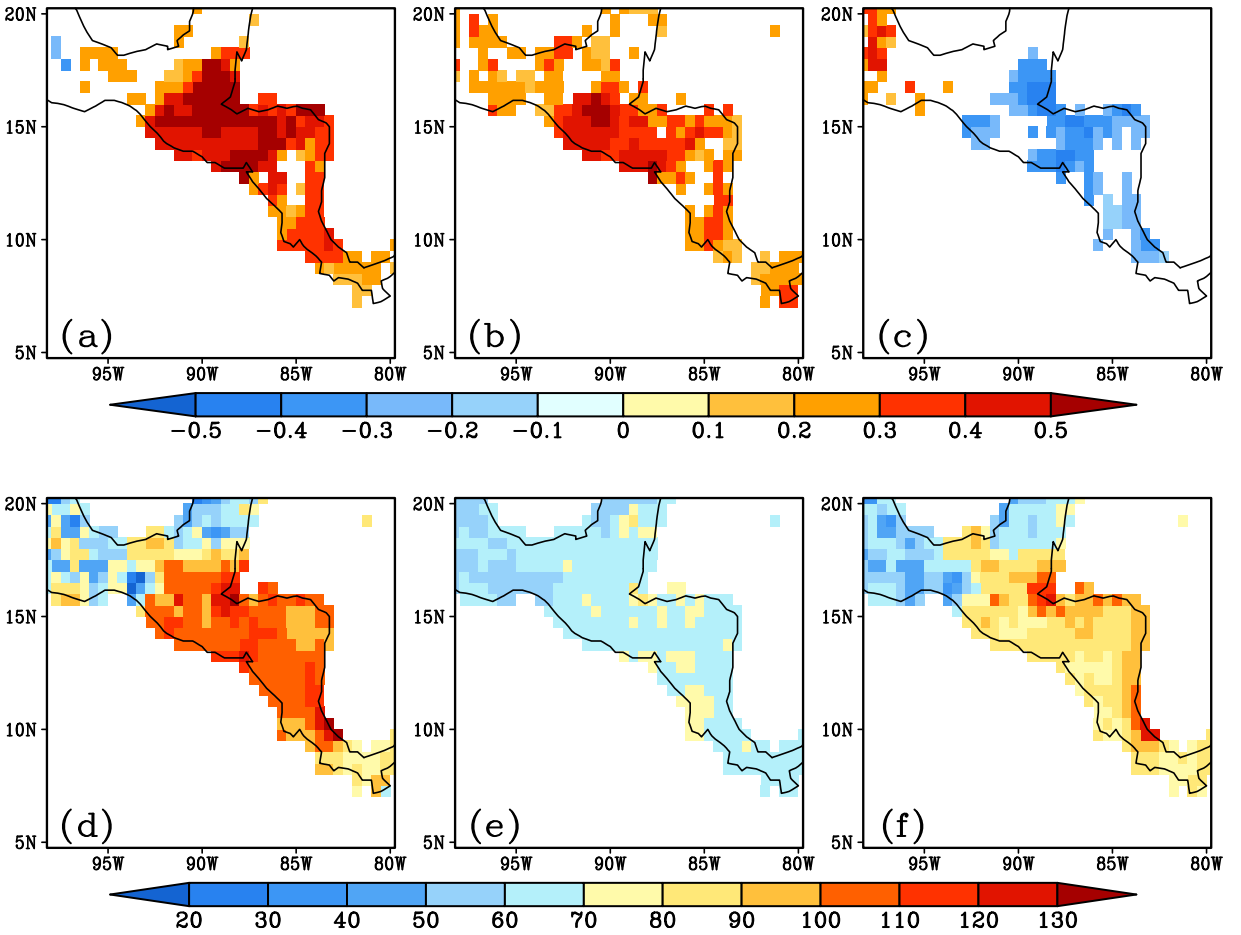

Figure 7. Correlation of the variability of the onset date of the AWP season with the (a) onset of the rainy season, (b) demise of the rainy season, and (c) length of the rainy season. Only significant values at 90% confidence interval are shown. The standard deviation of (a) onset, (b) demise dates, and (c) length of the rainy season over Mesoamerica in days.

following seasonal ASO rainfall variability in Central America, northern parts of South America, Caribbean region, and over a region extending from the southern Mississippi valley to the midwestern US east of Iowa. The onset date of the AWP also affects the onset and demise of the rainy season of Mesoamerica. The onset date variations of the AWP are also shown to be related to the following seasonal Atlantic tropical cyclone activity. With a relatively large variability of the onset date of AWP characterized by a relatively large range over the 34-year period (1979–2012) of the analysis ranging from April 27 (earliest) to August 7 (latest), it offers an ideal metric to monitor and anticipate the related seasonal rainfall anomalies with sufficient lead time. A caveat of this study is that we have not removed the apparent linear trend in the variations of the onset (Figure 3a) and demise (Figure 3b) dates of the AWP as a result of the relatively short length of the data record used in this study, which may have an influence on some of the teleconnections discussed in this paper.

Acknowledgments

This work was supported by grants from NOAA (NA12OAR4310078, NA10OAR4310215, NA11OAR4310110), and USDA (027865). Data used in this study are available on request from the authors.

References

Chan, S., V. Misra, and H. Smith (2009), A modeling study of the interaction between the Atlantic warm pool, the tropical Atlantic easterlies, and the Lesser Antilles. *J. Geophys. Res.*, *116*, D00Q02, doi:10.1029/2010JD015260.

Diro, G. T., S. A. Rauscher, F. Giorgi, A. M. Tompkins (2012), Sensitivity of seasonal climate and diurnal precipitation over Central America to land and sea surface schemes in RegCM4, *Clim. Res.*, *52*, 31–48.

Efron B., and R. J. Tibshirani (1993), *An Introduction to the Bootstrap*, vol. 436, Chapman and Hall, London.

Karnauskas, K. B., R. Seager, A. Giannini, and A. J. Busalacchi (2013), A simple mechanism for the climatolgoical midsummer drought along the Pacific coast of Central America, *Atmosfera*, *26*(2), 261–281.

Kelly, P., and B. E. Mapes (2011), Zonal mean wind, the Indian monsoon, and July drying in the western Atlantic subtropics, *J. Geophys. Res.*, *116*, D00Q07, doi:10.1029/2010JD015405.

Lee, S.-K., D. B. Enfield, and C. Wang (2007), What drives seasonal onset and decay of the western hemisphere warm pool? *J. Clim.*, *20*, 2133–2146.
Lee, S.-K., C. R. Mechoso, C. Wang, and J. D. Neelin (2013), Interhemispheric influence of the northern summer monsoons on the southern subtropical anticyclones. *J. Clim.*, *26*, 10193–10204, doi:10.1175/JCLI-D-13-00106.1.
Liebmann B., S. J. Carmargo, A. Seth, J. A. Marengo, L. M. V. Carvalho, D. Allured, R. Fu, C. S. Vera (2007), Onset and end of the rainy season in South America in observations and the ECHAM 4.5 atmospheric general circulation model, *J. Clim.*, *20*, 2037–2050.
Magaña, V. and E. Caetano (2005), Temporal evolution of summer convective activity over the Americas warm pools. *Geophys. Res. Lett.*, *32*, L02803, doi:10.1029/2004GL021033.
Magaña, V., J. Amador, and S. Medina (1999), The mid-summer drought over Mexico and central America, *J. Clim.*, *12*, 1577–1588.
Mapes, B. E., P. Liu, and N. Buenning (2005), Indian monsoon onset and the Americas midsummer drought: Out-of-equilibrium responses to smooth seasonal forcing, *J. Clim.*, *18*, 1109–1115.
McClave J. T., and F. H. Dietrich II (1994), *Statistics*, 967 pp., MacMillan, N. Y.
Misra, V. and S. DiNapoli (2012), The observed teleconnection between the equatorial Amazon and the Intra-Americas Seas, *Clim. Dyn.*, *40*, 2637–2649, doi:10.1007/s00382-012-1474-1.
Misra, V. and S. DiNapoli (2013), The variability of the Southeast Asian summer monsoon, *Int. J. Clim.*, *34*, 893–901, doi:10.1002/joc.3735.
Misra, V., L. Moeller, L. Stefanova, S. Chan, J. J. O'Brien, T. J. Smith III, and N. Plant (2011), The influence of Atlantic warm pool on Panhandle Florida Sea Breeze. *J. Geophys. Res.*, *116*, D00Q06, doi:10.1029/2010JD015367.
Misra, V., A. Stroman, and S. DiNapoli (2012), The rendition of the Atlantic warm pool in the reanalyses, *Clim. Dyn.*, *41*, 517–532, doi: 10.1007/s00382-012-1503-0.
Saha, S., et al. (2010), The NCEP climate forecast system reanalysis, *Bull. Am. Meteorol. Soc.*, *91*, 1015–1057.
Small, R. J. O., S. P. de Szoeke, and S. Xie (2007), The central American mid-summer drought: Regional aspects and large-scale forcing, *J. Clim.*, *20*, 4853–4873.
Wang, C., and D. B. Enfield (2001), The tropical western hemisphere warm pool, *Geophys. Res. Lett.*, *28*, 1635–1638, doi:10.1029/2000GL011763.
Wang, C., and D. B. Enfield (2003), A further study of the tropical western hemisphere warm pool, *J. Clim.*, *6*, 1476–1493.
Wang, C., and S. -K. Lee (2007), Atlantic warm pool, Caribbean low-level jet, and their potential impact on Atlantic hurricanes, *Geophys. Res. Lett.*, *34*, L02703, doi:10.1029/2006GL028579.
Wang, C., D. B. Enfield, S. -K. Lee, and C. Landsea (2006), Influences of the Atlantic warm pool on Western Hemisphere summer rainfall and Atlantic hurricanes, *J. Clim.*, *19*, 3011–3028.
Wang, C., S. -K. Lee, and D. B. Enfield (2008a), Climate response to anomalously large and small Atlantic Warm pools during the summer, *J. Clim.*, *21*, 2437–2450.
Wang, C., S.-K. Lee, and D. B. Enfield (2008b), Atlantic warm pool acting as a link between Atlantic multidecadal oscillation and Atlantic tropical cyclone activity, *Geochem. Geophys. Geosyst.*, *9*, Q05V03.
Wang, C., S.-K. Lee, and C. R. Mechoso (2010), Interhemispheric influence of the Atlantic warm pool on the southeastern Pacific, *J. Clim.*, *23*, 404–418.
Weisberg, R. H. (1996), On the evolution of SST over the PACS region, Abstracts of 76 'h AMS Annual Meeting, Am. Meteorol. Soc., Atlanta, Georgia, 378.
Xie, S. -P., H. Xu, W. S. Kessler, and M. Nonaka (2005) Air-sea interaction over the eastern Pacific warm pool: Gap winds, thermocline dome, and atmospheric convection, *J. Clim.*, *18*, 5–20.